

# A hybrid open-framework structure: synthesis and structure of an iron phosphate oxalate, $[\text{C}_{10}\text{N}_4\text{H}_{28}][\text{Fe}_2(\text{HPO}_4)_3(\text{C}_2\text{O}_4)]_2$

Amitava Choudhury<sup>a,b</sup> and Srinivasan Natarajan<sup>\*a</sup>

<sup>a</sup>Advanced Materials Research Laboratory, Chemistry and Physics of Materials Unit, Jawaharlal, Nehru Centre for Advanced Scientific Research, Jakkur P. O., Bangalore 560 064, India. E-mail: raj@jncasr.ac.in; Fax: + (080)-846-2766

<sup>b</sup>Solid State and Structural Chemistry Unit, Indian Institute of Science, Bangalore 560 064, India

Received 17th August 1999, Accepted 27th September 1999

A new inorganic–organic hybrid structure has been synthesized hydrothermally in the iron phosphate oxalate family using 1,4-bis(3-aminopropyl)piperazine as the structure-directing agent. Crystal data for **I**,  $[\text{C}_{10}\text{N}_4\text{H}_{28}][\text{Fe}_2(\text{HPO}_4)_3(\text{C}_2\text{O}_4)]_2$ :  $M = 589.8$ , monoclinic, space group =  $P2_1/n$  (no. 14),  $a = 10.829(1)$ ,  $b = 12.747(1)$ ,  $c = 12.397(1)$  Å,  $\beta = 95.1(1)^\circ$ ,  $V = 1704.4(3)$  Å<sup>3</sup>,  $Z = 4$ ,  $R = 0.036$  and  $R_w = 0.083$  [1860 observed reflections with  $I > 2\sigma(I)$ ]. The structure comprises a network of  $\text{FeO}_6$  octahedra and  $\text{PO}_4$  tetrahedra forming inorganic layers which are bridged by the oxalate units forming 8-membered channels in which the amine molecule resides. Magnetic susceptibility studies indicate an antiferromagnetic behavior with  $T_N \approx 40$  K, the highest known in an open-framework material.

## Introduction

The area of open framework solids continues to be of interest not only because of the novelty of the structures but also due to their potential applications in the areas of catalysis, sorption and separation processes.<sup>1</sup> Large numbers of materials with open architectures have been isolated in recent years and studied extensively.<sup>2</sup> Of the many open-framework solids that have been made and characterized, metal phosphates especially those of the transition metals form an important class of materials. Intense research during the last two years has resulted in the formation of large numbers of phosphates of iron,<sup>3–5</sup> cobalt<sup>6–8</sup> and nickel.<sup>9</sup> These materials are normally synthesized under hydrothermal conditions in the presence of a structure-directing agent. Framework materials containing dicarboxylate and metal ions have been made and characterized in recent years.<sup>10–15</sup> It is also established that oxalates substitute readily for phosphates in some of the open-framework structures and examples of such materials exist in the literature.<sup>16–18</sup> It has been shown recently<sup>19</sup> that in the phosphate oxalates the oxalate units generally cross-link the inorganic layers and act like a bridge. In this article we describe a new iron phosphate oxalate,  $[\text{C}_{10}\text{N}_4\text{H}_{28}][\text{Fe}_2(\text{HPO}_4)_3(\text{C}_2\text{O}_4)]_2$  **I**, possessing inorganic layers made from  $\text{FeO}_6$  octahedra and  $\text{PO}_4$  tetrahedra, bridged by oxalate units. The structure-directing amine is present in 8-membered channels formed by these linkages.

## Experimental

The iron phosphate oxalate **I** was synthesized starting from a mixture containing 1,4-bis(3-aminopropyl)piperazine (APPIP) as the structure directing agent. In a typical synthesis, 0.456 g of iron chloride was dispersed in 6 ml of water and 0.388 g of phosphoric acid (aq. 85 wt.%) was added with stirring. 0.213 g of oxalic acid and 0.34 ml of APPIP were added with continuous stirring and the mixture was homogenized for  $\approx 30$  min. The final composition of the mixture was:  $1.0\text{FeCl}_3 \cdot 6\text{H}_2\text{O} : 2.0\text{H}_3\text{PO}_4 : 1.0\text{H}_2\text{C}_2\text{O}_4 : 1.0\text{APPIP} : 200\text{H}_2\text{O}$ . All the chemicals were from Aldrich and used without any further purification. The starting mixtures were transferred and

sealed in a 23 ml capacity PTFE-lined stainless steel autoclave (Parr, Moline, IL, USA). The initial pH of the mixture was close to 2.0. The sealed pressure bombs were heated at 150 °C for 68 h under autogenous pressure. The reaction mixture after the above heat treatment did not show any appreciable change in the pH. The resulting product predominantly contained large quantities of crystals suitable for single crystal X-ray diffraction, which were filtered off and washed thoroughly with deionized water. The powder X-ray diffraction (XRD) pattern of the single crystals indicated that the product was a new material; the pattern was entirely consistent with the structure determined by single-crystal X-ray diffraction. A least squares fit of the powder XRD ( $\text{Cu-K}\alpha$ ) lines, using the  $hkl$  indices garnered from single crystal X-ray data, gave the cell parameters  $a = 10.818(1)$ ,  $b = 12.735(1)$ ,  $c = 12.385(2)$  Å,

**Table 1** X-Ray powder data for **I**,  $[\text{C}_{10}\text{N}_4\text{H}_{28}][\text{Fe}_2(\text{HPO}_4)_3(\text{C}_2\text{O}_4)]_2$

$h$	$k$	$l$	$d_{\text{obs}}/\text{Å}$	$d_{\text{calc}}/\text{Å}$	$I_{\text{rel}}$
1	0	-1	8.5090	8.5079	100.0
1	0	1	7.7867	7.7867	42.72
0	0	2	6.1650	6.1739	11.14
0	2	1	5.6580	5.6634	85.68
2	0	0	5.3990	5.3931	33.30
2	0	-2	4.2390	4.2538	31.07
1	0	-3	3.9590	3.9650	40.95
2	0	2	3.8940	3.8933	4.56
1	0	3	3.7290	3.7361	60.81
3	0	-1	3.5350	3.5378	28.87
0	2	3	3.4530	3.4576	13.10
0	4	0	3.1850	3.1866	86.04
3	1	-2	3.1340	3.1355	5.51
0	0	4	3.0870	3.0869	13.46
1	4	-1	2.9786	2.9842	28.82
3	2	-2	2.8800	2.8846	16.91
3	0	-3	2.8308	2.8360	7.46
4	0	0	2.6948	2.6966	13.94
2	0	4	2.5789	2.5817	11.98
2	4	-2	2.5471	2.5504	7.82
4	2	-1	2.4733	2.4743	9.72
1	4	3	2.4244	2.4245	5.42
4	0	2	2.3900	2.3941	5.06
1	0	5	2.3617	2.3619	2.28

**Table 2** Crystal data and structure refinement parameters of **I**

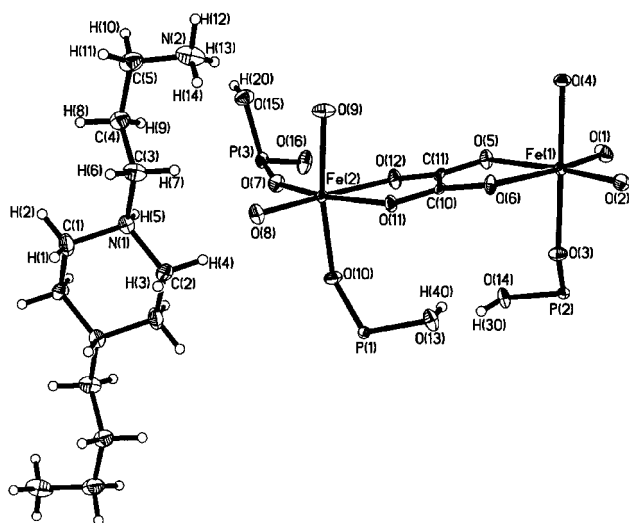
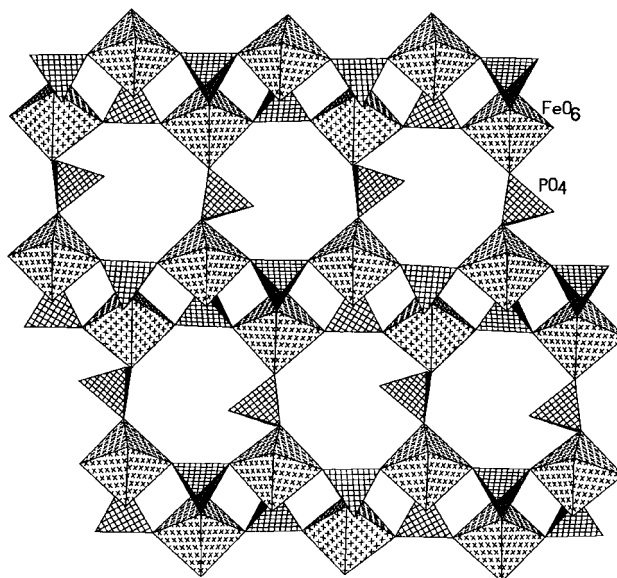
Empirical formula	Fe <sub>2</sub> P <sub>3</sub> O <sub>16</sub> C <sub>7</sub> N <sub>2</sub> H <sub>17</sub>
Crystal system	Monoclinic
Space group	<i>P</i> 2 <sub>1</sub> / <i>n</i> (no. 14)
<i>T</i> /K	298
<i>a</i> /Å	10.829(1)
<i>b</i> /Å	12.747(1)
<i>c</i> /Å	12.397(1)
$\beta$ /°	95.1(1)
<i>V</i> /Å <sup>3</sup>	1704.4(3)
<i>Z</i>	4
Formula mass	589.8
$\mu$ /mm <sup>-1</sup>	1.56
Total data collected	6935
Unique data	2445
Observed data [ <i>I</i> > 2 $\sigma$ ( <i>I</i> )]	1860
<i>R</i> <sub>int</sub>	0.041
<i>R</i> , <i>R</i> <sub>w</sub> [ <i>I</i> > 2 $\sigma$ ( <i>I</i> )	0.036; 0.083
(all data)	0.056; 0.091

$\beta = 95.07^\circ$ , which is in good agreement with those determined by single crystal XRD. Powder data for **I**, [C<sub>10</sub>N<sub>4</sub>H<sub>28</sub>][Fe<sub>2</sub>(HPO<sub>4</sub>)<sub>3</sub>(C<sub>2</sub>O<sub>4</sub>)<sub>2</sub>], are listed in Table 1. Thermogravimetric analysis (TGA) was carried out under a nitrogen atmosphere in the range from 25 to 700°C. Magnetic susceptibility measurements were carried out in the 20–300 K range using a Lewis coil magnetometer in a field of 0.5 tesla.

A suitable single crystal of compound **I** was carefully selected under a polarizing microscope and glued to a thin glass fiber. Crystal structure determination by X-ray diffraction was performed on a Siemens Smart-CCD diffractometer.

The structure was solved by direct methods using SHELXS 86<sup>20</sup> and Fourier difference syntheses. The hydrogen positions were initially located in the Fourier difference maps and for the final refinement the hydrogen atoms were placed geometrically and held in the riding mode. The last cycles of refinement included atomic positions for all the atoms, anisotropic thermal parameters for all non-hydrogen atoms and isotropic thermal parameters for all the hydrogen atoms. Full-matrix least-squares refinement against  $|F^2|$  was carried out using the SHELXTL PLUS<sup>21</sup> suite of programs. Details of the final refinements are given in Table 2. The final atomic coordinates, selected bond distances and bond angles are given for **I** in Tables 3–5.

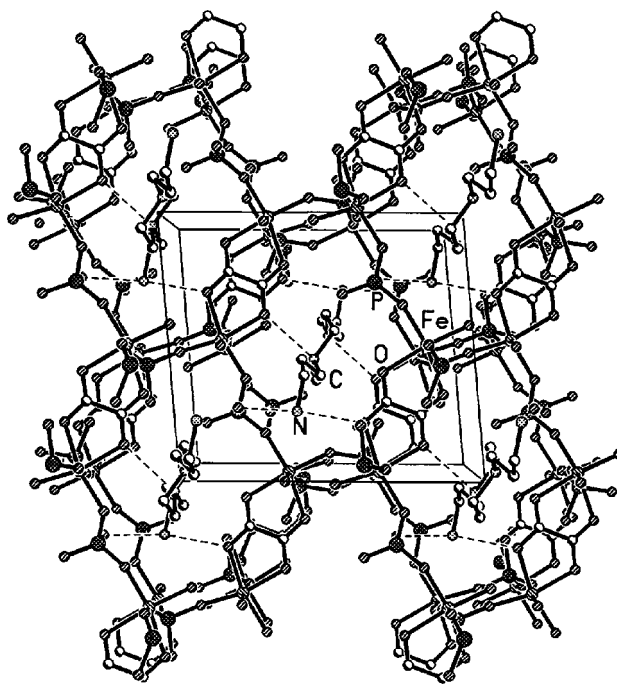
CCDC 1145/186. See <http://www.rsc.org/suppdata/jm/1999/3113> for crystallographic files in .cif format.

**Fig. 1** ORTEP plot of **I**, [C<sub>10</sub>N<sub>4</sub>H<sub>28</sub>][Fe<sub>2</sub>(HPO<sub>4</sub>)<sub>3</sub>(C<sub>2</sub>O<sub>4</sub>)<sub>2</sub>]. The asymmetric unit is labeled. Thermal ellipsoids are given at 50% probability.**Fig. 2** Polyhedral view of the structure of **I** along the *bc* plane showing the inorganic layers. Note that the ladder-like arrangement is connected by a phosphate group forming an 8-membered aperture.

## Results and discussion

The asymmetric unit of **I** contains 30 non-hydrogen atoms (Fig. 1). The structure consists of layers of formula [Fe<sub>2</sub>(HPO<sub>4</sub>)<sub>3</sub>], which are cross-linked by oxalate units forming the framework, which is anionic. Charge neutrality is achieved by the incorporation of the tetraprotonated organic structure-directing agent, 1,4-bis(3-aminopropyl)piperazine. There are 0.5[C<sub>10</sub>N<sub>4</sub>H<sub>28</sub>]<sup>4+</sup> molecules present per framework formula. The structure consists of a network of FeO<sub>6</sub>, PO<sub>4</sub> and C<sub>2</sub>O<sub>4</sub> moieties with each Fe atom bound to six oxygens, which are, in turn, bound to carbon and phosphorus atoms forming the network. Conversely, the oxalate ions cross-link the inorganic layers formed by the linkage between the FeO<sub>6</sub> octahedra and PO<sub>4</sub> tetrahedra.

The framework structure of **I** is made from layers bridged by

**Fig. 3** Structure of **I** along *b* axis showing the oxalate bridges and the amine molecules. The linkages form an 8-membered channel.

**Table 3** Atomic coordinates [ $\times 10^4$ ] and equivalent isotropic displacement parameters [ $\text{\AA}^2 \times 10^3$ ] for **I**

Atom	X	Y	Z	U(eq) <sup>a</sup>
Fe(1)	298(1)	8790(1)	6592(1)	9(1)
Fe(2)	5095(1)	8751(1)	8522(1)	8(1)
P(1)	4344(1)	11234(1)	8814(1)	9(1)
P(2)	707(1)	11274(1)	6077(1)	9(1)
P(3)	7480(1)	8398(1)	6969(1)	13(1)
O(1)	-194(3)	8864(2)	5087(2)	18(1)
O(2)	-1242(3)	8880(2)	7305(2)	15(1)
O(3)	483(3)	10316(2)	6764(2)	14(1)
O(4)	59(3)	7221(2)	6607(2)	13(1)
O(5)	2137(3)	8663(2)	6224(2)	13(1)
O(6)	1284(3)	8682(2)	8143(2)	12(1)
O(7)	6631(3)	8660(2)	7828(3)	16(1)
O(8)	5853(3)	8693(2)	9998(2)	15(1)
O(9)	4828(3)	7223(2)	8403(3)	18(1)
O(10)	5105(3)	10296(2)	8515(3)	15(1)
O(11)	3224(3)	8797(2)	8940(2)	12(1)
O(12)	4075(3)	8821(2)	6984(2)	15(1)
O(13)	2978(3)	11151(2)	8243(3)	18(1)
O(14)	2158(3)	11401(2)	6051(3)	18(1)
O(15)	7669(3)	7151(2)	7028(3)	20(1)
O(16)	7019(3)	8716(3)	5844(3)	23(1)
C(10)	2444(4)	8734(3)	8139(4)	9(1)
C(11)	2940(4)	8740(3)	7019(4)	9(1)
C(1)	10659(5)	9128(4)	10500(4)	26(1)
C(2)	8685(4)	9871(4)	9740(4)	21(1)
N(1)	9536(4)	8954(3)	9712(3)	15(1)
C(3)	8915(5)	7915(4)	9893(4)	22(1)
C(4)	9538(5)	7058(4)	9314(4)	25(1)
C(5)	8935(5)	5988(4)	9346(4)	27(1)
N(2)	7582(4)	5997(3)	9022(4)	30(1)

<sup>a</sup>Defined as one third of the trace of the orthogonalized  $U_{ij}$  tensor.

oxalate units. The inorganic layers are formed along the *bc* plane by the linkages between the 4-membered ladder-like edge-shared chains and a phosphate unit as shown in Fig. 2. This type of linkage within a sheet is common amongst the open-framework metal phosphates especially the aluminium phosphates.<sup>2</sup> Along the *b* axis, the oxalate units connect the iron centers from adjacent layers and act like pillars by cross-linking these layers as shown in Fig. 3. Thus, the oxalate units keep these inorganic layers apart and together. The other way to describe this structure is to view along the *ab* plane. Along

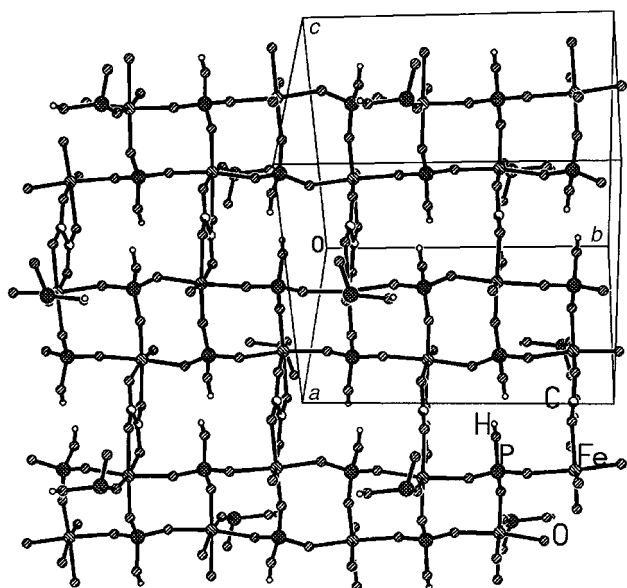


**Fig. 4** Structure of **I** along the *ab* plane showing the 4-membered ladders and the linkages *via* an oxalate unit. Note that the phosphate units hanging from the ladder-like arrangement extend to form the layer (Fig. 2).

**Table 4** Selected bond lengths ( $\text{\AA}$ ) in **I**

Fe(1)–O(1)	1.896(3)	Fe(1)–O(2)	1.959(3)
Fe(1)–O(3)	1.965(3)	Fe(1)–O(4)	2.017(3)
Fe(1)–O(5)	2.089(3)	Fe(1)–O(6)	2.119(3)
Fe(2)–O(7)	1.943(3)	Fe(2)–O(8)	1.939(3)
Fe(2)–O(9)	1.972(3)	Fe(2)–O(10)	1.969(3)
Fe(2)–O(11)	2.135(3)	Fe(2)–O(12)	2.118(3)
P(1)–O(8) <sup>a</sup>	1.509(3)	P(1)–O(10)	1.517(3)
P(1)–O(4) <sup>b</sup>	1.527(3)	P(1)–O(13)	1.586(3)
P(2)–O(1) <sup>c</sup>	1.510(3)	P(2)–O(9) <sup>a</sup>	1.511(3)
P(2)–O(3)	1.520(3)	P(2)–O(14)	1.583(3)
P(3)–O(16)	1.495(3)	P(3)–O(7)	1.506(3)
P(3)–O(2) <sup>d</sup>	1.537(3)	P(3)–O(15)	1.604(3)
C(10)–O(6)	1.258(5)	C(10)–O(11)	1.248(5)
C(11)–O(5)	1.259(5)	C(11)–O(12)	1.238(5)
C(10)–C(11)	1.532(7)		
Organic moiety			
N(1)–C(1)	1.507(6)	C(1)–C(2) <sup>e</sup>	1.503(7)
C(2)–N(1)	1.491(6)	N(1)–C(3)	1.510(6)
C(3)–C(4)	1.500(7)	C(4)–C(5)	1.514(7)
C(5)–N(2)	1.484(7)		

<sup>a</sup>–*x*+1, –*y*+2, –*z*+2. <sup>b</sup>–*x*+1, *y*+1, –*z*+3. <sup>c</sup>–*x*, –*y*+2, –*z*+1. <sup>d</sup>*x*+1, *y*, *z*. <sup>e</sup>–*x*+2, –*y*+2, –*z*+2.

the *ab* plane the 4-membered edge-shared ladders possessing a pendant phosphate group are linked *via* the oxalate units as shown in Fig. 4. The pendant phosphate groups are connected to another such ladder completing the architecture. The structure-directing amine molecule, 1,4-bis(3-aminopropyl)-piperazine, occupies the 8-membered channels formed by the linkages between these units and interacts with the framework *via* the oxygens.

Of the six oxygens bound to iron, four are associated with Fe–O distances in the range 1.896–2.017  $\text{\AA}$  [ $\text{Fe}(1)_{\text{ave}}$  1.959;  $\text{Fe}(2)_{\text{ave}}$  1.956  $\text{\AA}$ ] and the other two with distances of 2.089–2.135  $\text{\AA}$ . These are the oxygens linked to phosphorus and

**Table 5** Selected bond angles ( $^\circ$ ) in **I**

O(1)–Fe(1)–O(2)	105.4(1)	O(8)–Fe(2)–O(7)	96.2(1)
O(1)–Fe(1)–O(3)	94.3(1)	O(8)–Fe(2)–O(10)	92.3(1)
O(2)–Fe(1)–O(3)	88.6(1)	O(7)–Fe(2)–O(10)	93.0(1)
O(1)–Fe(1)–O(4)	91.9(1)	O(8)–Fe(2)–O(9)	94.5(1)
O(2)–Fe(1)–O(4)	86.5(1)	O(7)–Fe(2)–O(9)	91.9(1)
O(3)–Fe(1)–O(4)	172.9(1)	O(10)–Fe(2)–O(9)	171.1(1)
O(1)–Fe(1)–O(5)	88.8(1)	O(8)–Fe(2)–O(12)	173.7(1)
O(2)–Fe(1)–O(5)	165.8(1)	O(7)–Fe(2)–O(12)	90.1(1)
O(3)–Fe(1)–O(5)	90.6(1)	O(9)–Fe(2)–O(12)	85.1(1)
O(4)–Fe(1)–O(5)	92.9(1)	O(10)–Fe(2)–O(12)	87.5(1)
O(1)–Fe(1)–O(6)	166.1(1)	O(8)–Fe(2)–O(11)	95.9(1)
O(2)–Fe(1)–O(6)	88.9(1)	O(7)–Fe(2)–O(11)	167.6(1)
O(3)–Fe(1)–O(6)	85.9(1)	O(9)–Fe(2)–O(11)	84.8(1)
O(4)–Fe(1)–O(6)	88.9(1)	O(10)–Fe(2)–O(11)	88.8(1)
O(5)–Fe(1)–O(6)	77.3(1)	O(12)–Fe(2)–O(11)	77.7(1)
O(8) <sup>a</sup> –P(1)–O(10)	114.5(2)	O(8) <sup>a</sup> –P(1)–O(4) <sup>b</sup>	112.6(2)
O(10)–P(1)–O(4) <sup>b</sup>	108.1(2)	O(8) <sup>a</sup> –P(1)–O(13)	103.4(2)
O(10)–P(1)–O(13)	110.1(2)	O(4) <sup>b</sup> –P(1)–O(13)	108.0(2)
O(1) <sup>c</sup> –P(2)–O(9) <sup>b</sup>	112.2(2)	O(1) <sup>c</sup> –P(2)–O(3)	112.2(2)
O(9) <sup>b</sup> –P(2)–O(3)	108.6(2)	O(1) <sup>c</sup> –P(2)–O(14)	105.9(2)
O(9) <sup>b</sup> –P(2)–O(14)	110.2(2)	O(3)–P(2)–O(14)	107.6(2)
O(16)–P(3)–O(7)	115.2(2)	O(16)–P(3)–O(2) <sup>d</sup>	111.3(2)
O(7)–P(3)–O(2) <sup>d</sup>	108.2(2)	O(16)–P(3)–O(15)	110.0(2)
O(7)–P(3)–O(15)	105.7(2)	O(2) <sup>d</sup> –P(3)–O(15)	106.0(2)
O(6)–C(10)–O(11)	127.3(4)	O(5)–C(11)–O(12)	126.7(4)
Organic moiety			
C(1)–N(1)–C(2)	109.5(3)	N(1)–C(1)–C(2) <sup>e</sup>	110.9(4)
C(1)–N(1)–C(3)	112.3(4)	C(2)–N(1)–C(3)	113.6(4)
N(1)–C(3)–C(4)	110.0(4)	C(3)–C(4)–C(5)	115.5(5)
C(4)–C(5)–N(2)	113.8(4)		

<sup>a</sup>–*x*+1, –*y*+2, –*z*+2. <sup>b</sup>–*x*+1, *y*+1, –*z*+3. <sup>c</sup>–*x*, –*y*+2, –*z*+1. <sup>d</sup>*x*+1, *y*, *z*. <sup>e</sup>–*x*+2, –*y*+2, –*z*+2.

**Table 6** Important hydrogen bond interactions (distances in Å, angles in °) in **I**

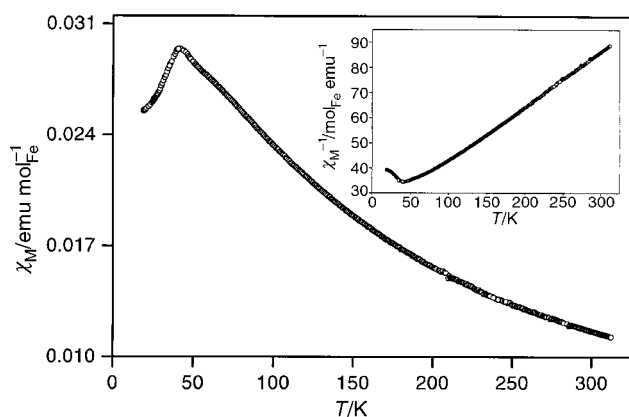
O(2)⋯H(5)	2.339(1)	O(2)–H(5)–N(1)	132.5(2)
O(6)⋯H(5)	2.054(1)	O(6)–H(5)–N(91)	146.1(1)
O(16)⋯H(12)	2.213(1)	O(16)–H(12)–N(2)	138.8(1)
O(15)⋯H(13)	2.040(1)	O(15)–H(13)–N(2)	158.0(2)
O(5)⋯H(14)	2.188(2)	O(5)–H(14)–N(2)	130.4(1)
O(7)⋯H(4)	2.576(1)	O(7)–H(4)–C(2)	152.6(1)
O(12)–H(6)	2.600(1)	O(12)–H(6)–C(3)	140.6(2)
O(16)⋯H(8)	2.398(1)	O(16)–H(8)–C(4)	154.4(1)
O(4)⋯H(9)	2.530(2)	O(4)–H(9)–C(4)	160.3(1)
O(12)⋯H(11)	2.440(2)	O(12)–H(11)–C(5)	143.2(2)
O(4)⋯H(20) <sup>a</sup>	2.064(1)	O(4)–H(20)–O(15)	132.6(1)
O(13)⋯H(30) <sup>a</sup>	2.020(1)	O(13)–H(30)–O(14)	158.9(2)
O(14)⋯H(40) <sup>a</sup>	2.071(2)	O(14)–H(40)–O(13)	148.1(1)

<sup>a</sup>Intraframework.

carbon atoms respectively. Similar bond distances have been observed before. The O–Fe–O bond angles are in the range 77.3–173.7° [ $\text{Fe}(1)_{\text{ave}}$  105.6,  $\text{Fe}(2)_{\text{ave}}$  106°] which are in agreement with those seen earlier. The P–O distances and O–P–O bond angles are also as expected. Similar structural parameters have been observed for C–O and O–C–O bond distances and angles as well. Bond valence sum calculations<sup>22</sup> indicate that one of the oxygens attached to each phosphorus atom [O(13), O(14), O(15)] has a hydrogen atom attached to it making it a terminal OH group and one oxygen [O(16)] attached to P(3) is a terminal double bonded oxygen. These structural parameters are in the range expected for this type of bonding.

Thermogravimetric analysis carried out under a N<sub>2</sub> atmosphere in the temperature range 25–700 °C indicated one sharp mass loss with a broad tail. The sharp mass loss of 24.2% occurring at 350 °C may correspond to loss of the amine molecules (calc. 21%) as well as the beginning of the loss of oxalates from the framework. The mass loss of about 15% in the region 350–650 °C indicates the oxalates start leaving the solid at more or less at the same time as that of the amine molecules. The total mass loss of 39.2% corresponds with the loss of amine and oxalate from the solid (calc. 41.2%). The calcined sample showed a weakly diffracting XRD pattern with the majority of the lines corresponding to the crystalline phase Fe<sub>4</sub>(P<sub>2</sub>O<sub>7</sub>)<sub>3</sub> [JCPDS: 36-0318].

The importance of hydrogen bonding in open-framework materials has been emphasized before and the current solid also possesses important interactions involving the amine molecules and the framework. In addition, strong intra-framework hydrogen bond interactions are also observed. Selected hydrogen bond interactions in **I** are listed in Table 6. As can be seen, the terminal OH groups and double bonded oxygen

**Fig. 5** Variation of magnetic susceptibility as a function of temperature showing the antiferromagnetic behavior of **I**. Inset shows the inverse susceptibility vs. temperature plot.

(=O) take an active part in hydrogen bonding with the amine molecules. These interactions might lend additional structural stability to this material.

In Fig. 5 the variation of magnetic susceptibility as a function of temperature is presented. The studies indicate the presence of strong antiferromagnetic interactions ( $\theta_p = -88$  K) and the solid orders antiferromagnetically at  $T_N = 40$  K. The paramagnetic region (300–50 K) obeys the Curie–Weiss law with a magnetic moment of 5.99  $\mu_B$ , which agrees well with the spin-only magnetic moment of Fe<sup>III</sup> (5.98  $\mu_B$ ).

The co-ordination environment of iron atoms in phosphates and oxalates presents an interesting comparison. While in most of the phosphate based open-framework structures iron is present in either five- or six-co-ordination forming a trigonal bipyramidal FeO<sub>5</sub> or octahedral FeO<sub>6</sub> as the building units, in oxalates<sup>14</sup> and oxalate phosphates<sup>16–19</sup> including the present solid iron is present exclusively in an octahedral environment. This, we believe, is because the average charge per oxygen on the oxalate (0.5) is less than that on the phosphate (0.75), such that more oxalate oxygens are needed to satisfy the valence of iron.

## Conclusion

The synthesis and structure of a novel open-framework hybrid iron phosphate oxalate possessing iron phosphate layers and oxalate bridges has been demonstrated. The FeO<sub>6</sub> octahedra and PO<sub>4</sub> tetrahedra alternate strictly within the layer forming 4- and 8-membered apertures akin to those seen in aluminophosphates. The Neel temperature of  $\approx 40$  K is one of the highest obtained in this type of materials especially so where the iron sub-network is zero-dimensional as in the present case. This opens up the entire area of magnetic performance of the porous solids.

## Acknowledgements

The authors thank Professor C. N. R. Rao, FRS for his kind support and encouragement. One of us (A.C.) thanks the Council of Scientific and Industrial Research (CSIR), Govt. of India for the award of a research fellowship.

## References

- 1 *Handbook of Heterogeneous Catalysis*, eds. G. Ertl, H. Knözinger and J. Weitkamp, VCH, Berlin, 1997.
- 2 A. K. Cheetham, T. Loiseau and G. Ferey, *Angew. Chem., Int. Ed.*, 1999 (in press).
- 3 K.-H. Lii, Y.-F. Huang, V. Zima, C.-Y. Huang, H.-M. Lin, Y.-C. Jiang, F.-L. Liao and S.-L. Wang, *Chem. Mater.*, 1998, **10**, 2599 and refs. therein.
- 4 A. Choudhury, S. Natarajan and C. N. R. Rao, *Chem. Commun.*, 1999, 1305; A. Choudhury and S. Natarajan, *Proc. Indian Natl. Acad. (Chem. Sci.)*, 1999 (in press).
- 5 M. Cavellec, D. Riou and G. Ferey, *J. Solid State Chem.*, 1994, **112**, 441; M. Cavellec, D. Riou, J.-M. Greneche and G. Ferey, *Zeolites*, 1996, **17**, 252; M. Cavellec, C. Egger, J. Linares, M. Nogues, F. Varret and G. Ferey, *J. Solid State Chem.*, 1997, **134**, 349; M. R. Cavellec, J.-M. Greneche, D. Riou and G. Ferey, *Chem. Mater.*, 1998, **10**, 2434.
- 6 P. Feng, X. Bu and G. D. Stucky, *Nature (London)*, 1997, **388**, 735; X. Bu, P. Feng and G. D. Stucky, *Science*, 1997, **278**, 2080; P. Feng, X. Bu, S. H. Tolbert and G. D. Stucky, *J. Am. Chem. Soc.*, 1997, **119**, 2497.
- 7 J. Chen, R. H. Jones, S. Natarajan, M. B. Hursthouse and J. M. Thomas, *Angew. Chem., Int. Ed. Engl.*, 1994, **33**, 639; N. Zabukovec, L. Golic, P. Fajdiga and P. Kaucic, *Zeolites*, 1995, **15**, 104.
- 8 A. M. Chippindale and A. R. Cowley, *J. Chem. Soc., Dalton Trans.*, 1999, 2147; *Zeolites*, 1997, **18**, 176.; A. M. Chippindale, A. R. Cowley and R. I. Walton, *J. Mater. Chem.*, 1996, **6**, 611; J. R. D. DeBord, R. C. Haushalter and J. Zubieta, *J. Solid State Chem.*, 1996, **125**, 270; J. R. D. DeBord, W. M. Reiff, R. C. Haushalter and J. Zubieta, *J. Solid State Chem.*, 1996,

- 125, 186; J. R. D. DeBord, W. M. Reiff, C. J. Warran, R. C. Haushalter and J. Zubieta, *Chem. Mater.*, 1997, **9**, 1994.
- 9 N. Guillou, Q. Gao, M. Nogues, R. E. Morris, M. Hervieu, G. Ferey and A. K. Cheetham, *C.R. Acad. Sci. Paris, Ser. II*, 1999, 387.
- 10 F. Serpaggi and G. Ferey, *J. Mater. Chem.*, 1998, **8**, 2737; C. Livage, C. Egger, M. Nogues and G. Ferey, *J. Mater. Chem.*, 1998, **8**, 2743; A. Distler and S. C. Sevov, *Chem. Commun.*, 1998, 959.
- 11 S. O. H. Gutschke, M. Molinier, A. K. Powell and P. T. Wood, *Angew. Chem., Int. Ed. Engl.*, 1997, **36**, 991; S. Romero, A. Mosset and J. C. Trombe, *Eur. J. Solid State Inorg. Chem.*, 1997, **34**, 209; V. Kiritsis, A. Michaelides, S. Skoulika, S. Golhen and L. Ouahab, *Inorg. Chem.*, 1998, **37**, 3407.
- 12 S. Drumel, P. Janvier, P. Barboux, M. Bujoli-Doeuff and B. Bujoli, *Inorg. Chem.*, 1995, **34**, 148; S. Drumel, P. Janvier, M. Bujoli-Doeuff and B. Bujoli, *New. J. Chem.*, 1995, **19**, 239.
- 13 S. Decurtins, H. W. Schmalle, H. R. Oswald, A. Linden, J. Ensling, P. Gütllich and A. Hauser, *Inorg. Chim. Acta.*, 1994, **216**, 65; *J. Am. Chem. Soc.*, 1994, **116**, 9521.
- 14 H. Tamaki, Z. J. Zhong, N. Matsumoto, S. Kida, M. Koikawa, N. Achiwa, Y. Hashimoto and H. Okawa, *J. Am. Chem. Soc.*, 1992, **114**, 6974; C. Mathoniere, S. G. Carling and P. Day, *J. Chem. Soc., Chem. Commun.*, 1994, 1551; M. Clemente-Leon, E. Coronado, J.-R. Galán-Mascarós and C. J. Gómez-García, *Chem. Commun.*, 1997, 1727 and refs. therein.
- 15 S. Ayyappan, A. K. Cheetham, S. Natarajan and C. N. R. Rao, *Chem. Mater.*, 1998, **10**, 3746; S. Natarajan, R. Vaidyanathan, C. N. R. Rao, S. Ayyappan and A. K. Cheetham, *Chem. Mater.*, 1999, **11**, 1633.
- 16 S. Natarajan, *J. Solid State Chem.*, 1998, **139**, 200.
- 17 Z. A. D. Lethbridge and P. Lightfoot, *J. Solid State Chem.*, 1999, **143**, 58; P. Lightfoot, Z. A. D. Lethbridge, R. E. Morris, D. S. Wragg, P. A. Wright, Å. Kvik and G. B. M. Vaughan, *J. Solid State Chem.*, 1999, **143**, 74.
- 18 Y.-F. Huang and K.-H. Lii, *J. Chem. Soc., Dalton Trans.*, 1998, 4085; H.-M. Lin, K.-H. Lii, Y.-C. Jiang and S.-L. Wang, *Chem. Mater.*, 1999, **11**, 519.
- 19 A. Choudhury, S. Natarajan and C. N. R. Rao, *J. Solid State Chem.*, 1999, **146**, 538; A. Choudhury, S. Natarajan and C. N. R. Rao, *Chem. Mater.*, 1999, **11**, 2316.
- 20 G. M. Sheldrick, SHELXS 86, Program for Crystal Structure Determination, University of Göttingen, 1986; *Acta Crystallogr., Sect. A*, 1990, **35**, 467.
- 21 G. M. Sheldrick, SHELXTL PLUS, Program for Crystal Structure Solution and Refinement, University of Göttingen, 1993.
- 22 I. D. Brown and D. Altermatt, *Acta Crystallogr., Sect. B*, 1984, **41**, 244.

Paper 9/06663B